Toward high-energy laser-driven ion beams: Nanostructured double-layer targets

M. Passoni,[1,2,*] A. Sgattoni,[3] I. Prencipe,[1,4] L. Fedeli,[1,3,5] D. Dellasega,[1,2] L. Cialfi,[1] Il Woo Choi,[6,7,†] I Jong Kim,[6,7,‡] K. A. Janulewicz,[6,8,9] Hwang Woon Lee,[6] Jae Hee Sung,[6,7] Seong Ku Lee,[6,7] and Chang Hee Nam[6,8]

[1]*Dipartimento di Energia, Politecnico di Milano, Milan 20133, Italy*
[2]*Istituto di Fisica del Plasma, Consiglio Nazionale delle Ricerche, research unit "Piero Caldirola", Milan 20125, Italy*
[3]*Istituto Nazionale di Ottica, Consiglio Nazionale delle Ricerche, research unit "Adriano Gozzini", Pisa 56124, Italy*
[4]*Institut für Strahlenphysik, Helmholtz–Zentrum Dresden–Rossendorf, Dresden 01328, Germany*
[5]*Dipartimento di Fisica "Enrico Fermi", Università di Pisa, Pisa 56127, Italy*
[6]*Center for Relativistic Laser Science, Institute for Basic Science, Gwangju 61005, Korea*
[7]*Advanced Photonics Research Institute, Gwangju Institute of Science and Technology, Gwangju 61005, Korea*
[8]*Department of Physics and Photon Science, Gwangju Institute of Science and Technology, Gwangju 61005, Korea*
[9]*Institute of Optoelectronics, Military University of Technology, 00-908 Warsaw, Poland*

(Received 23 October 2015; published 20 June 2016)

The development of novel target concepts is crucial to make laser-driven acceleration of ion beams suitable for applications. We tested double-layer targets formed of an ultralow density nanostructured carbon layer (~7 mg/cm^3, 8–12 μm–thick) deposited on a μm–thick solid Al foil. A systematic increase in the total number of the accelerated ions (protons and C^{6+}) as well as enhancement of both their maximum and average energies was observed with respect to bare solid foil targets. Maximum proton energies up to 30 MeV were recorded. Dedicated three-dimensional particle-in-cell simulations were in remarkable agreement with the experimental results, giving clear indication of the role played by the target nanostructures in the interaction process.

DOI: 10.1103/PhysRevAccelBeams.19.061301

Laser-driven ion acceleration may become an appealing alternative to conventional acceleration techniques for a number of scientific and technological applications which require high-energy ion beams and compact sources [1,2]. In such a scheme, ions are accelerated by the strong electric fields (>1 MV μm^{-1}) generated during the interaction of ultrahigh-intensity laser pulses (well above 10^{18} W/cm^2) with dense targets, typically thin solid foils (0.01–10 μm-thick). Currently, laser-driven ion acceleration allows one to obtain bunches in a broad range of energies (1–70 MeV for protons) and promises to envision new ion sources with reduced radioprotection requirements in comparison to traditional accelerators. However, in order to be appealing for applications, further increase in both the maximum ion energy and the accelerated charge is mandatory. Moreover, most applications require an ion beam with average currents of nA, μA or even mA. Up to now these issues have been addressed separately. In the last few years several target concepts have been developed with the aim of increasing the maximum ion energy: ultrathin foils [3,4], reduced mass targets [5], nanosphere targets [6–8], and grating targets [9]. Recently energies up to 20 MeV/u for C^{6+} ions and 29 MeV for protons were obtained using ultrathin diamond-like carbon (DLC) foils covered with a layer of carbon nanotubes [10]. Most of these targets and the related acceleration schemes are suitable to work only in single-shot mode, besides requiring ultrahigh pulse contrast. For the generation of an ion beam it is necessary to work in a repetitive regime, for example with Ti:sapphire laser systems (1–10 Hz). Only few works can be found in which sequences of laser-driven ion bunches are generated, using μm-thick foils or tapes, showing modest maximum energies (about 4 MeV with a 100 TW system) [11,12]. Therefore, the crucial task to obtain suitable ion energies and beam currents is inevitably related to the development of novel smart target concepts apt to be employed in the repetitive regime and able to provide,

*matteo.passoni@polimi.it
†iwchoi@gist.ac.kr
‡Present address: Optical Instrumentation Development Team, Korea Basic Science Institute (KBSI), 169-148 Gwahak-ro, Yuseong-gu, Daejeon 34133, Republic of Korea.

at the same time, an improvement in acceleration performances in terms of maximum ion energy and accelerated charge. Targets having an ultralow-density layer (*foam*) deposited on the front surface of a μm-thick solid foil may represent a promising path to meet both the aforementioned requirements. Idealized models of this target configuration have recently been investigated via particle-in-cell (PIC) simulations [13,14]. These studies revealed that the presence of a homogeneous plasma (ionized foam) with near-critical electron density ($n_e \sim n_c = (m_e\omega^2)/(4\pi e^2)$, where ω is the laser frequency, and e and m_e are the charge and the electron mass) may strongly enhance both number and energy of the accelerated ions. This density regime is characterized by strong laser–plasma coupling [10,15–18]. A sizeable number of electrons from the low-density plasma is accelerated toward the rear side of the target [13], strongly contributing to the sheath field and, as a consequence, to the enhancement of the ion acceleration. Experimentally, near-critical plasmas can be produced from materials characterized by an open nanostructure resulting in a low density at the macroscale. Besides technological relevance, this target design is therefore of interest also for revealing the fundamental mechanisms characterizing interaction between ultraintense laser pulses and nanostructured materials [19]. Preliminary experimental results for laser-driven ion acceleration with carbon foam-attached targets, performed at moderate intensities ($<10^{18}$ W/cm^2), showed an increase of both the energy and number of accelerated ions, without strong laser contrast requirements [15].

In this paper we report the results of an experimental investigation of the carbon foam–attached target concept in the fully relativistic regime. The experiments were performed at the Center for Relativistic Laser Science (CoReLS), Institute for Basic Science (IBS) in Korea, operating a 30-fs, petawatt Ti:sapphire laser [20]. The energies of the accelerated ions were measured as a function of laser polarization and intensity. The results were interpreted on the basis of three-dimensional particle-in-cell (3D-PIC) simulations including innovative features to describe the nanostructured foam plasma layer. The experimental setup is shown in Fig. 1. Double-layer targets (DLT) were composed by a 0.75 μm-thick Al foil and a near-critical carbon foam layer (7 ± 0.7 mg/cm^3, corresponding to $n_e = 1.2\ n_c$ when fully ionized) with 8 μm or 12 μm thickness. The carbon foam was directly grown on the Al substrate using pulsed laser deposition (PLD) (see Refs. [21,22] for details). An innovative method based on energy dispersive x-ray spectroscopy combined with cross section scanning electron microscopy was employed to evaluate carbon foam density [23]. The laser pulses delivered on target had energy between 1 J to 7.4 J, duration of 30 fs, and a focal spot of 5 μm containing 22% of the total pulse energy in the FWHM area. Thus, the available intensity ranged from 0.5 to 4.5×10^{20} W/cm^2. A double plasma mirror system [24] allows one to maintain

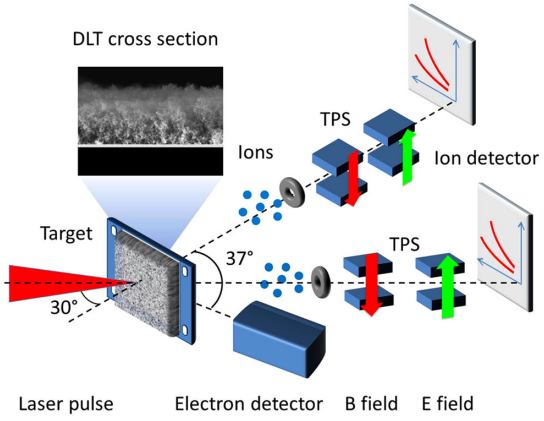

FIG. 1. Setup of the experiment. The laser pulse is tightly focused by an off-axis parabolic mirror (angle of incidence 30°) onto 8 or 12 μm–thick carbon foam deposited on a 0.75 μm–thick Al foil. Ion spectra are recorded using two Thomson parabola spectrometers (TPS) and electron spectra are collected with an electron spectrometer.

a high temporal contrast, better than 10^{-11} up to tens of ps before the main pulse. Laser polarization was changed between linear (s–, p–) and circular (c–) by using half- and quarter-wave plates, leading to slightly different maximum intensities. The targets were irradiated with an incidence angle of 30°. For DLT, the foam layer was positioned on the irradiated target surface. Two Thomson parabola spectrometers were used to measure the energy spectra of ions emitted along both the target normal and the laser propagation direction from the target rear surface. The ion traces were detected using a high dynamic (16-bit) CCD camera coupled with a microchannel plate and a phosphor screen. An electron spectrometer was also positioned at the rear side of the target at an angle of 37° from the target normal. The electron spectra in the 2–11 MeV energy range were measured using imaging plates (Fujifilm, BAS-SR).

The measured proton spectra, shown in Fig. 2, were obtained for the cases of 8 μm-thick DLT and for the bare 0.75 μm-thick solid Al foil target (ST) used as a reference. The maximum energy of accelerated protons ($E_p^{\max}$) was 22, 18 and 10 MeV for ST under laser irradiation with p-, s-, and c-polarization, respectively. The variation in the proton energies is due to the strong dependence of the laser-solid interaction mechanisms on the laser polarization at oblique incidence [25]. On the contrary, for DLT, the measured $E_p^{\max}$ was almost independent of the laser polarization and approached a value of 30 MeV. The corresponding gain factors were in the range 1.4–3. A further confirmation that the laser-foam interaction is hardly sensitive to the laser polarization came from the analysis of the electron spectra using 12 μm-thick DLT and ST for s- and c- polarizations, reported in the inset of Fig. 2. It can be seen that almost identical electron spectra were observed for different laser polarizations when DLTs are used. On the other hand, laser polarization strongly affects

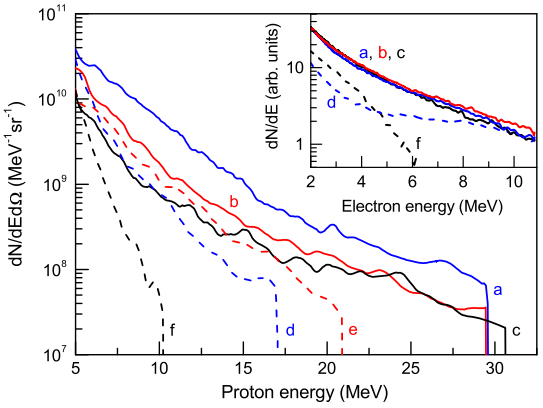

FIG. 2. Energy spectra of the protons obtained with a laser intensity of 4.1, 3.5, 3.7×10^{20} W/cm^2 for s-, p- and c–polarization respectively. The targets are DLT with 8 μm–thick foam (spectra a, b, c respectively) and ST (spectra d, e and f). The spectra are collected along the target normal direction. The inset shows the electron energy spectra when using DLT with 12 μm–thick foam with s–, p- and c–polarization, (spectra a, b, c respectively) and using ST for s–and c–polarization (spectra d and f).

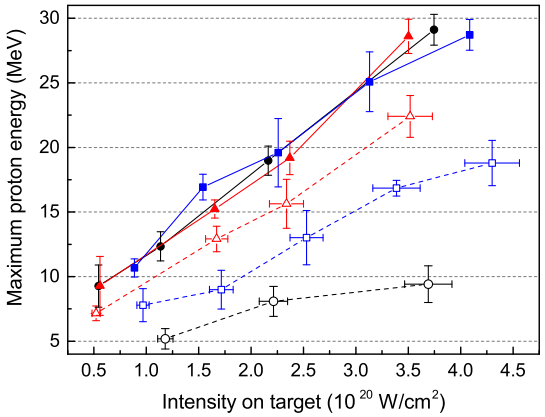

FIG. 3. Role of laser polarization and intensity. $E_p^{\max}$ as a function of laser intensity with s- (blue squares), p- (red triangles), and c-polarization (black circles) for ST (empty symbol) and DLT with 8 μm–thick foam (full symbol). Horizontal error bars are reported only for the ST case to improve the clarity of the graph.

the electron spectra obtained using ST. Parallel to this, maximum energy of about 130 MeV (∼11 MeV/u) was obtained for C^{6+} ions using 8 μm–thick DLT, while only 80 MeV were observed for ST. The data presented in Fig. 2 allow a comparison of the total number of protons per steradian (N_p) and the total energy of the proton bunch per steradian (E_T), considering only ions with energies > 8 MeV, produced with DLT and ST respectively. The strong increase in both N_p and E_T is evident for DLT. The gain factors for E_T and N_p are 10 and 9 for s-polarization, 2 and 2 for p-polarization and 30 and 21 for c-polarization, respectively. The presence of the foam layer allowed a very strong increase in the number of the high-energy ions. In particular, in the case of p-polarization the number of protons with energy above 18 MeV was 7 times greater for DLT than for ST while no protons above 18 MeV could be found for s- and c-polarization using ST. Also the role played by the Al substrate thickness has been investigated. The presence of the foam allows the use of thicker substrates without substantially affecting $E_p^{\max}$. Differently from the well-known behavior of ST [2], doubling the Al thickness for DLT does not affect $E_p^{\max}$. Preliminary results from a more recent campaign suggest that high $E_p^{\max}$ may be obtained even using much thicker Al foils: 20 MeV protons were obtained using a 12 μm–thick Al foil DLT irradiated at quasinormal incidence with c–polarization and 20% more energy on target. In Fig. 3, $E_p^{\max}$ is shown as a function of the laser intensity for s-, p-, and c-polarization, for the cases of DLT and ST. An enhancement in $E_p^{\max}$ from the DLT, when compared to ST, was observed in the whole intensity range. The maximum proton energy increases approximately linearly as a function of the laser intensity, irrespectively of the polarization. This is valid for both the DLTs for all the polarizations, and for the ST with the exception of c-polarization. Such a behavior in the case of ST is in agreement with available theoretical predictions [26,27].

The experimental results presented so far are in qualitative agreement with the predictions of the simplified model used in numerical simulations described in Refs. [13–15]. In these simulations (mainly 2D) the foam layer was considered as a homogeneous near-critical layer. 3D simulations are essential to reproduce ion energies in quantitative agreement with the experiments and to assess the effect of different pulse polarizations. Moreover, since the deposited carbon foam consists of dense nanoparticles aggregated in a random structure [21] it is important to assess how the foam structure may additionally influence the laser-target coupling. Therefore, dedicated 3D–PIC simulations were performed with the PIC code PICCANTE [28] simulating both a uniform near-critical layer and a more realistic nanostructured foam [22]. The latter was modeled as a material composed by a random collection of 50 nm–radius overdense ($n = 50n_c$) plasma nanoparticles. The randomness of the arrangement has been achieved by adopting the diffusion limited aggregation model [29,30]. The initial configuration is shown in Fig. 4(a). The resulting porous structure is characterized by an occupation factor of about 2%, consistent with an average electron density over the entire foam volume approximately equal to n_c. Figure 4(b) and Fig. 4(c) show the electron density evolving by interaction with a p-polarized laser at two different moments. The simulations show that the laser propagates through the entire nanostructured layer. An almost uniform electron density is achieved after about 130 fs (after the laser-target interaction is concluded), implying that during the laser-target interaction the plasma has modulations at the micrometer scale. During the interaction volumetric heating occurs, and the pulse is

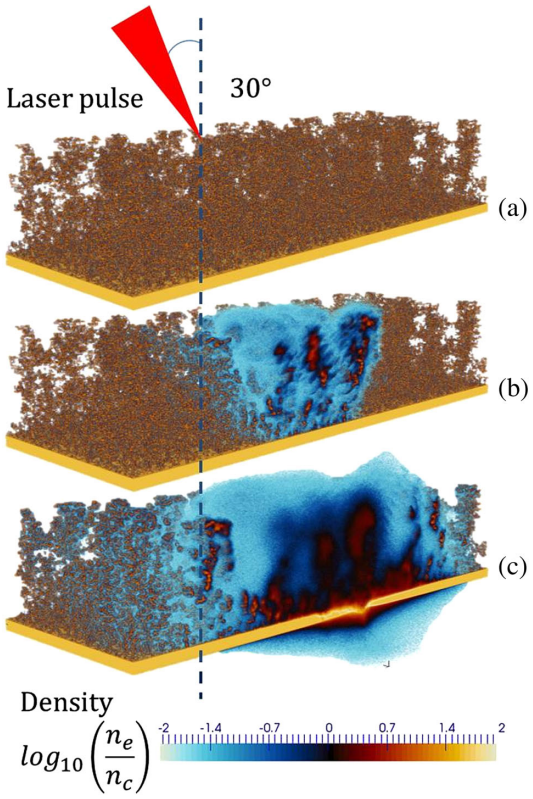

FIG. 4. 3D–PIC simulations of the electron density dynamics in the interaction between a laser pulse and a nanostructured foam at different times: (a) 0 fs, (b) 67 fs, and (c) 134 fs. The red cone represents the incident laser, and the yellow layer indicates Al substrate.

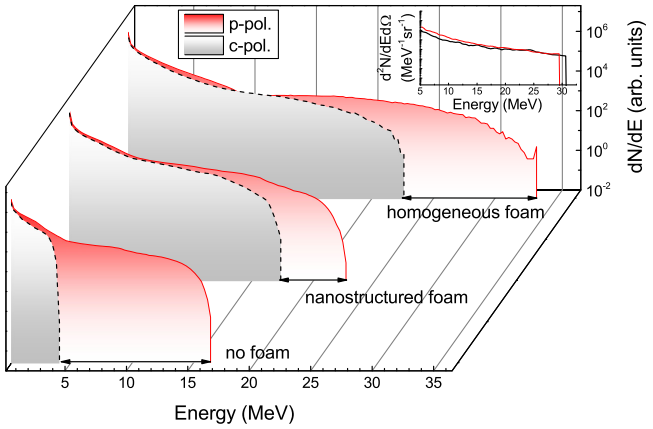

FIG. 5. Calculated proton energy spectra from homogeneous foam, nanostructured foam, and Al foil using p- and c- polarized laser pulse. The inset shows the corresponding experimental spectra.

strongly absorbed by the electrons of the foam, which are accelerated to relativistic velocities in the forward direction and reach the rear side of the solid target. Thus ion acceleration is due to an enhanced target normal sheath acceleration (TNSA) process. A similar dynamics was observed from the simulation performed with a c-polarized laser (not shown). The corresponding proton spectra, obtained after 170 fs, are shown in Fig. 5 in comparison with those obtained with the model of homogenous foam and bare Al target for both p- and c-polarization. Using either the homogeneous near-critical layer or the nanostructured foam we observed an increase in both $E_p^{\max}$ and N_p with respect to Al target. The simulations with the uniform layer show a strong polarization dependence of the ion spectra while the presence of a nanostructured foam strongly reduces the differences between the two investigated polarizations, as observed in the experiment. This may be due to the nanostructure since the laser-plasma interaction occurs with a quasirandom set of angles of incidence. Although the calculated maximum proton energies for the nanostructured foam are underestimated compared to the experimental values, the computed gain factors (1.4 and 3.8 for p- and c-polarization, respectively) are in very good agreement with the experiment (1.4 and 3).

It is also interesting to compare our results with those obtained by Bin *et al.* [10], in which effective ion acceleration is achieved by exploiting laser interaction with a near-critical density plasma, thanks to the use of ultrathin DLC foils covered by a layer of carbon nanotubes (CNT). In this study, the ion acceleration is ascribed to an enhanced light-sail radiation pressure acceleration (LS-RPA) mechanism, in which the laser pulse is self-focused in the propagation through the near-critical CNT layer. In our experiment the use of oblique incidence and micrometer-thick solid foils excludes the onset of LS-RPA, favoring instead an enhanced TNSA process characterized by laser polarization independence (see Fig. 3) and volumetric heating within the foam, which therefore plays an active role in coupling the laser energy to the charged particles. A further remarkable experimental outcome emerged from the ion spectra acquired along the laser propagation direction (see Fig. 1). Only when DLTs were used, protons with $E_p^{\max}$ ranging between 12–14 MeV were detected. $E_p^{\max}$ was almost constant in the whole intensity range and independent on both foam thickness and laser polarization. We may speculate that these ions, rather than being accelerated on the rear side by a sheath field, are coming from the foam layer.

According to the results presented above, the enhanced coupling of the laser with near-critical carbon foam layer allows for a significant improvement in the performance of laser-driven ion acceleration, when compared to ST. The recorded ion energies and gain factors are among the highest obtained with comparable sets of laser parameters [4,7,10,31,32]. As a remarkable distinctive feature, these energies are obtained with DLT having μm-thick Al foils. Thus it is possible to envisage the use of this target design in repetitive regime for the generation of laser-driven ion beams (e.g. with a rotating support [33]). Proton beams with energy in the 10–30 MeV may already find application

in several fields [34–37]. Further enhancement could be obtained by optimizing foam parameters, for example by further reducing the average foam density [13,15]. In addition, the experiment was performed using laser pulses of few-J and well below 10^{21} W/cm^2. These values can be realistically overcome with today's available laser technology. Considering the trend of the maximum ion energy as a function of laser intensity (see Fig. 2) significantly higher $E_p^{\max}$ might be reached beyond 10^{21} W/cm^2.

In conclusion, thanks to the robustness of μm–thick foil and to the enhanced laser-target coupling, foam-based multilayer targets may represent a promising solution toward the development of repetitive laser-driven ion beams.

The authors wish to thank A. Macchi. This work was supported by Institute for Basic Science under IBS-R012-D1 in Korea, and under the framework of international cooperation program managed by National Research Foundation of Korea (NRF-2013K2A1B8074481), and by the GRI (GIST Research Institute) National Research Council (Agreement CNR/NRF, Joint Projects 2014-2015). The research leading to these results has also received funding from the European Research Council Consolidator Grant ENSURE (ERC-2014-CoG No. 647554). We also acknowledge ISCRA and LISA access schemes to the BlueGene/Q machine FERMI at CINECA, Italy, via the projects "LaCoSA" (ISCRA) and "LAPLAST" (LISA).

[1] H. Daido, M. Nishiuchi, and A. S. Pirozhkov, Review of laser-driven ion sources and their applications, Rep. Prog. Phys. **75**, 056401 (2012).

[2] A. Macchi, M. Borghesi, and M. Passoni, Ion acceleration by superintense laser-plasma interaction, Rev. Mod. Phys. **85**, 751 (2013).

[3] A. Henig *et al.*, Radiation-Pressure Acceleration of Ion Beams Driven by Circularly Polarized Laser Pulses, Phys. Rev. Lett. **103**, 245003 (2009).

[4] I J. Kim *et al.*, Transition of Proton Energy Scaling Using an Ultrathin Target Irradiated by Linearly Polarized Femtosecond Laser Pulses, Phys. Rev. Lett. **111**, 165003 (2013).

[5] S. Buffechoux *et al.*, Hot Electrons Transverse Refluxing in Ultraintense Laser-Solid Interactions, Phys. Rev. Lett. **105**, 015005 (2010).

[6] D. Margarone *et al.*, Laser-Driven Proton Acceleration Enhancement by Nanostructured Foils, Phys. Rev. Lett. **109**, 234801 (2012).

[7] D. Margarone *et al.*, Laser-driven high-energy proton beam with homogeneous spatial profile from a nanosphere target, Phys. Rev. ST Accel. Beams **18**, 071304 (2015).

[8] V. Floquet *et al.*, Micro-sphere layered targets efficiency in laser driven proton acceleration, J. Appl. Phys. **114**, 083305 (2013).

[9] T. Ceccotti *et al.*, Evidence of Resonant Surface-Wave Excitation in the Relativistic Regime through Measurements of Proton Acceleration from Grating Targets, Phys. Rev. Lett. **111**, 185001 (2013).

[10] J. H. Bin *et al.*, Ion Acceleration Using Relativistic Pulse Shaping in Near-Critical-Density Plasmas, Phys. Rev. Lett. **115**, 064801 (2015).

[11] A. Yogo *et al.*, Measurement of relative biological effectiveness of protons in human cancer cells using a laser-driven quasimonoenergetic proton beamline, Appl. Phys. Lett. **98**, 053701 (2011).

[12] A. Yogo *et al.*, Development of laser-driven quasi-monoenergetic proton beam line for radiobiology, Nucl. Instrum. Methods Phys. Res., Sect. A **653**, 189 (2011).

[13] A. Sgattoni, P. Londrillo, A. Macchi, and M. Passoni, Laser ion acceleration using a solid target coupled with a low-density layer, Phys. Rev. E **85**, 036405 (2012).

[14] T. Nakamura, M. Tampo, R. Kodama, S. V. Bulanov, and M. Kando, Interaction of high contrast laser pulse with foam-attached target, Phys. Plasmas **17**, 113107 (2010).

[15] M. Passoni, A. Zani, A. Sgattoni, D. Dellasega, A. Macchi, I. Prencipe, V. Floquet, P. Martin, T. V. Liseykina, and T. Ceccotti, Energetic ions at moderate laser intensities using foam-based multi-layered targets, Plasma Phys. Controlled Fusion **56**, 045001 (2014).

[16] M. Borghesi *et al.*, Macroscopic Evidence of Soliton Formation in Multiterawatt Laser-Plasma Interaction, Phys. Rev. Lett. **88**, 135002 (2002).

[17] L. Willingale, P. M. Nilson, A. G. R. Thomas, S. S. Bulanov, A. Maksimchuk, W. Nazarov, T. C. Sangster, C. Stoeckl, and K. Krushelnick, High-power, kilojoule laser interactions with near-critical density plasma, Phys. Plasmas **18**, 056706 (2011).

[18] M. Borghesi, A. J. MacKinnon, L. Barringer, R. Gaillard, L. A. Gizzi, C. Meyer, O. Willi, A. Pukhov, and J. Meyer-ter-Vehn, Relativistic Channeling of a Picosecond Laser Pulse in a Near-Critical Preformed Plasma, Phys. Rev. Lett. **78**, 879 (1997).

[19] M. A. Purvis *et al.*, Relativistic plasma nanophotonics for ultrahigh energy density physics, Nat. Photonics **7**, 796 (2013).

[20] J. H. Sung, S. K. Lee, T. J. Yu, T. M. Jeong, and J. Lee, 0.1 Hz 1.0 PW Ti:sapphire laser, Opt. Lett. **35**, 3021 (2010).

[21] A. Zani, D. Dellasega, V. Russo, and M. Passoni, Ultra-low density carbon foams produced by pulsed laser deposition, Carbon **56**, 358 (2013).

[22] I. Prencipe *et al.*, Development of foam-based layered targets for laser-driven ion beam production, Plasma Phys. Controlled Fusion **58**, 034019 (2016).

[23] I. Prencipe, D. Dellasega, A. Zani, D. Rizzo, and M. Passoni, Energy dispersive x-ray spectroscopy for nanostructured thin film density evaluation, Sci. Technol. Adv. Mater. **16**, 025007 (2015).

[24] I. J. Kim, I. W. Choi, S. K. Lee, K. A. Janulewicz, J. H. Sung, T. J. Yu, H. T. Kim, H. Yun, T. M. Jeong, and J. Lee, Spatio-temporal characterization of double plasma mirror for ultrahigh contrast and stable laser pulse, Appl. Phys. B **104**, 81 (2011).

[25] P. Gibbon, *Short Pulse Laser Interactions with Matter* (Imperial College Press, London, 2005).

[26] M. Passoni, L. Bertagna, and A. Zani, Target normal sheath acceleration: theory, comparison with experiments and future perspectives, New J. Phys. **12**, 045012 (2010).

[27] A. Zani, A. Sgattoni, and M. Passoni, Parametric investigations of target normal sheath acceleration experiments, Nucl. Instrum. Methods Phys. Res., Sect. A **653**, 94 (2011).

[28] A. Sgattoni *et al.*, Optimising PICCANTE–an Open Source Particle-in-Cell Code for Advanced Simulations on Tier-0 Systems, PRACE white paper **1** (2015).

[29] T. A. Witten and L. M. Sander, Diffusion-Limited Aggregation, a Kinetic Critical Phenomenon, Phys. Rev. Lett. **47**, 1400 (1981).

[30] T. A. Witten and L. M. Sander, Diffusion-limited aggregation, Phys. Rev. B **27**, 5686 (1983).

[31] K. Zeil, S. D Kraft, S. Bock, M. Bussmann, T. E. Cowan, T. Kluge, J. Metzkes, T. Richter, R. Sauerbrey, and U. Schramm, The scaling of proton energies in ultrashort pulse laser plasma acceleration, New J. Phys. **12**, 045015 (2010).

[32] K. Ogura *et al.*, Proton acceleration to 40 MeV using a high intensity, high contrast optical parametric chirped-pulse amplification/Ti:sapphire hybrid laser system, Opt. Lett. **37**, 2868 (2012).

[33] A. Graham and C. Spindloe, in *Targetry for Laser–driven Proton (Ion) Accelerator Sources: First Workshop, Institute for Advanced Study (IAS), Garching, Germany* (2013).

[34] S. Mathew, T. K. Chan, D. Zhan, K. Gopinadhan, A. R. Barman, M. B. H. Breese, S. Dhar, Z. X. Shen, T. Venkatesan, and J. T. L. Thong, Mega-electron-volt proton irradiation on supported and suspended graphene: A Raman spectroscopic layer dependent study, J. Appl. Phys. **110**, 084309 (2011).

[35] M. J. Fluss, P. Hosemann, and J. Marian, *Charged-Particle Irradiation for Neutron Radiation Damage Studies. Characterization of Materials* (John Wiley and Sons, Inc., New York, 2012), ISBN: 9780471266969, pp. 1–17.

[36] M. Imaizumi *et al.*, *Photovoltaic Specialists Conference (PVSC), 38th IEEE* (Institute of Electrical and Electronics Engineers, Piscataway, 2012), ISBN: 978-1-4673-0064-3, p. 2831.

[37] *Nuclear Physics for Medicine*, edited by F. Azaiez *et al.* (European Science Foundation, Strasbourg, 2014), ISBN: 978-2-36873-008-9.